Calculations of fission rates for r-process nucleosynthesis. [1]

I.V.Panov [a,b,2] E.Kolbe [a] B.Pfeiffer [c] T.Rauscher [a] K.-L.Kratz [c]
F.-K. Thielemann [a]

[a] *University of Basel, Klingelbergstr. 82, CH-4056 Basel, Switzerland*

[b] *Institute for Theoretical and Experimental Physics, B.Cheremushkinskaya 25, Moscow, 117259, Russia.*

[c] *Institute fur Kernchemie, Fritz-Strassman-Weg 2, D-55128 Mainz, Germany*

Abstract

Fission plays an important role in the r-process which is responsible not only for the yields of transuranium isotopes, but may have a strong influence on the formation of the majority of heavy nuclei due to fission recycling. We present calculations of beta-delayed and neutron-induced fission rates, taking into account different fission barriers predictions and mass formulae. It is shown that an increase of fission barriers results naturally in a reduction of fission rates, but that nevertheless fission leads to the termination of the r-process. Furthermore, it is discussed that the probability of triple fission could be high for $A > 260$ and have an effect on the formation of the abundances of heavy nuclei. Fission after beta-delayed neutron emission is discussed as well as different aspects of the influence of fission upon r-process calculations.

Key words: fission; fission rates; r-process;
PACS: 21.10.Dr; 24.60.Dr; 24.75.+i; 25.85.Ec; 25.85.Ca; 26.30.+k

1 Introduction

Fission is an important process which is responsible not only for the yields of the transuranium isotopes in the r-process calculation and for termination of the r-process, but also for the formation of the majority of heavy nuclei due to cycling of the r-process from transuranium region into the region of A≈130

[1] Partially supported by Swiss National Fonds
[2] corresponding author: Igor.Panov@itep.ru

(where fission products are involved again in the r-process nucleosynthesis). For a consistent treatment of the r-process, we have to consider fission barriers based on the same mass formulae that are used for the calculation of other reaction rates and decay properties. We have to evaluate all fission branches: neutron-induced fission, beta-delayed fission and spontaneous fission. In addition, one should analyze the importance of every separate fission mode for the termination of the r-process, as well as nuclear abundance yields and the related age determination from the chronometer nuclei abundances.

The fission barriers, used in the past for fission rate calculations [1] were probably underestimated. Recent calculations [2,3] predict higher fission barriers, sometimes significantly. Therefore, a recalculation of fission rates is important as well as an evaluation of their sensitivity on nuclear data. We consider all fission channels, but first discuss beta-delayed and neutron-induced fission.

While the study of fission in the r-process has a long history [4], its main focus was related to cosmochronometers [5,6,7]. Only chronometer abundances are affected if the neutron freeze-out occurs when the r-process (in the envelope of a supernova) approaches the transuranium region and yields of fission products play small role for the abundances of all light r-process nuclei. For high neutron densities existing over long periods, fission cycling to lighter nuclei becomes important. For the latter case, considering only instantaneous fission is a first step towards a consistent treatment as performed in a number of recent studies: (a) $P_{fission} \equiv P_{sf} = 1$ for all A > 240 [8]; (b) $P_{fission} \equiv P_{sf} = 1$ for all A > 256 [6]; (c) for A $= 260$ [9]. In all these cases only a symmetric mass distribution was considered, while other calculations already included asymmetric mass distributions [4,7].

In the first extended calculation of beta-delayed fission for the majority of r-process nuclei [10], it turned out that the fission probability could reach 100% and beta-delayed fission affects strongly the transuranium yields, especially the yields of cosmochronometer nuclei. Their yields are used to determine the stellar age or the age of our galaxy as the lower limit on the age of the universe. For r-process conditions with long durations of high neutron densities, neutron-induced fission could also play an important role. That can be seen from the comparison of neutron-induced fission rates for uranium isotopes [11] employing the old barrier estimates [1] and extended calculations for a variety of fission barrier models [12]. The availability of new extended fission barrier calculations [2,13], requires that all the fission rates need to be reevaluated for the inclusion in r-process calculations.

The latest observations of metal-poor stars emphasize also the importance of the mass region $110 < A < 130$ for the understanding of the role of fission in the r-process. One notices that these nuclei are underabundant and the solar system r-process must have at least two components, the one dominating for

A<130 and the other one dominating for A>130 [14]. The observation of the second component in low metallicity stars and the observed abundances for A<130 might give strong clues to fission properties, if the explanation of the second component is related to an r-process site with a high neutron supply which leads to fission cycling. This should be investigated as the site of the r-process is still uncertain.

Here we want to emphasize that, besides neutron-induced fission and beta-delayed fission rates, the mass-distribution of fission yields is important as well as it was discussed earlier [15]. Although the mass distribution of fission products is known rather well for long-lived transactinide nuclei, the mass distribution after fission of neutron-rich heavy elements is an open question. The r-process yields in the mass region of $80 < A < 120$ can be affected by the mass distribution of fissioning nuclei, and triple or ternary [16] fission can play an important role in some cases.

Beta-delayed fission rates differ very strongly due to difficulties to predict reliable beta-strength functions for very neutron-rich and especially for deformed nuclei as well as reliable fission barriers for such nuclei.

In a number of calculations [10,17], (contrary to [18]) the values of beta-delayed fission probabilities for a large number of short-lived neutron-rich heavy nuclei can attain 100%, when applying the fission barriers of [1], (especially for transuranium nuclei) independent of beta-strength functions were used (see Fig. 1, Fig. 2). The beta-strength function S_β used in [10] was based on Tamm-Dancoff approximation for the Gamow-Teller residual interaction. Another calculation [17] used the proton-neutron Quasiparticle Random Phase Approximation (pn-QRPA) [19] with a shematic Gamow-Teller residual interaction. Three sets of calculations with 3 different mass formulae [1,20,22] were considered taking into account an implicit treatment of nuclear deformation.

Beta-delayed fission calculations for a number of selected nuclei were also performed [21] with a schematic consideration of deformations as in [17], to mix a basis of deformed nuclear states via the GT residual interaction. Fig. 1 shows some values of $P_{\beta df}$ with different parameterization of the β-strength-function (squares) and artificial overestimation (triangles) and underestimation (circles) of fission barriers and values from existing data sets [10,17] for the isotopes of Pa (Z=91). Both of the existing data sets [10,17] strongly depend on the β-strength function, mass models and fission barrier heights, and their application to r-process models gave quite different results [15].

The degree of difference depends on the r-process model used. In the case of the classical model of the r-process, the path of the r-process lies along nuclei with neutron separation energy $S_n \approx 2$MeV, and the r-process stops at mass numbers A≈260. Both of the data sets [10,17] yield the maximum

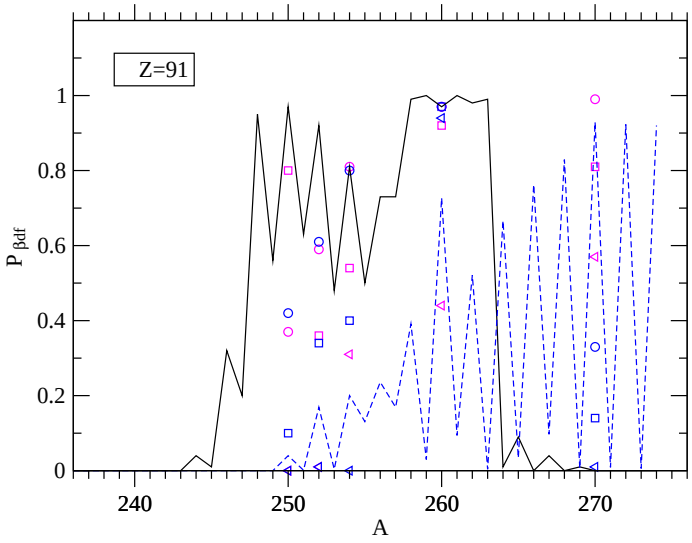

Fig. 1. The calculated probabilities for beta-delayed fission P_{bdf} for Pa- isotopes from different calculations using approach of Tamm-Dancoff [10] (line), QRPA [17] (dashed line) and RPA approximation with some artificial parametrization [21] (circles, squares and triangles).

values of $P_{\beta f}$ for these nuclei. That is why the previously used approximation of 100% instantaneous fission in the vicinity of A$\sim$260 [6], [9], [11] was a fairly good approximation. But when considering extreme r-process paths in the framework of the classical model ($S_n \sim 3$ MeV or $S_n \sim 1$ MeV) or with a calculation of the heavy element abundances in a very high neutron density environment, the difference in the results with utilization of different beta-delayed fission rates can be large.

It has to be noted that for very neutron rich nuclei the possibility of fission after delayed neutron emission could be rather high and, that in principle, such a fission mode also should be calculated. In Fig. 2, different calculations of the beta-delayed fission probabilities [10,17] with the same fission barriers [1] are compared, including the rates of fission after beta-delayed neutron emission. The strength-function dependence and the high values of $P_{n\beta df}$ are clearly seen, especially for heavy Cf-isotopes.

The details of the statistical approach will be introduced in Section 2, including a discussion of the beta-strength function and probability of fission after beta-delayed neutron emission. A comparison of different fission barriers and mass predictions used in present calculations is shown in Section 3. In Section 4 we present the results. The impact analysis and a comparison of the different decay modes in fission is discussed in subsection 4.1 with evaluations based on older mass predictions [22] and fission barriers [1], often used in astrophysical applications. In subsection 4.2, we discuss the fission rates for more recent nuclear physics input from the Thomas-Fermi [2] and ETFSI [13] models and discuss the changes. In Sections 5 and 6, the possible consequences of fission

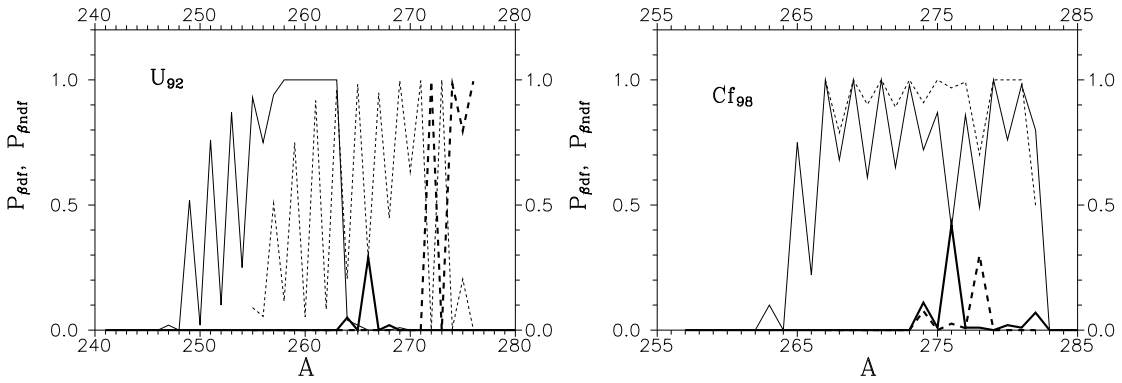

Fig. 2. Fission probabilities $P_{\beta df}$ (thin lines) and $P_{\beta ndf}$ (bold lines) for U and Cf isotopes for different strength-functions: Tamm-Dankoff [10] (lines) and pn-QRPA [17] (dashed lines). Mass predictions [22] and fission barriers of ref. [1] were used.

rates are considered: cycling of the r-process due to fission into the region of A≈130, and the influence of triple fission on the yields of medium mass nuclei.

2 The statistical approach to fission rates

As in previous approaches [10,17], we have applied the statistical Hauser-Feshbach formalism for the calculation of fission rates. It has been shown [23] that the statistical model is very well applicable for the astrophysical neutron-induced rate calculations, as long as there is a high density of excited states, which is the case for heavy nuclei. Of course, just near the neutron drip-line the systematic errors of the approach in neutron-induced fission rate calculations can rise, underlining that reliable mass predictions are absolutely necessary for r-process applications far from stability. Early r-process calculations made use of the mass predictions by Hilf et al. [22] and the fission barriers of ref. [1] for fission rate evaluations. For a consistent treatment of fission rates, however, the neutron separation energies, reaction Q-values and fission barrier heights should be used from the same mass model.

2.1 Neutron-Induced fission and beta-delayed fission

The cross-section for a neutron-induced reaction $i^0(n,f)$ from the target ground state i^0 with center of mass energy E_{in} and reduced mass μ_{in} is given by

$$\sigma_{nf}(E_{in}) = \frac{\pi\hbar^2/(2\mu_{in}E_{in})}{(2J_i^0+1)\cdot(2J_n+1)}\sum_{J,\pi}(2J+1)\frac{T_n^0(E,J^\pi,E_i^0,J_i^0,\pi_i^0)T_f(E,J^\pi)}{T_{\rm tot}(E,J^\pi)}. \quad (1)$$

The transition coefficient $T_f(E, J^\pi)$ includes the sum over all possible final states. Since the work of Strutinski [24] fission has been generally described within the framework of double-humped fission barriers. Similar to previous work [10] we followed this approximation of a two-hump barrier. The calculation of the fission probabilities was performed in the complete damping approximation which averages over transmission resonances, assuming that levels in the second minimum are equally spaced.

Then beta-delayed fission rate can be expressed by

$$\lambda_f = \int_0^{Q_\beta} \sum_i \beta_i(E, J_i, \pi_i) \cdot \frac{T_f(E, J_i, \pi_i)}{T_{\rm tot}(E, J_i, \pi_i)} dE \tag{2}$$

where the beta-feeds $\beta_i(E, J_i, \pi_i)$ are expressed via reduced transition probabilities $B(E, J_i, \pi_i)$, taking into account a Gauss spreading of states:

$$\beta_i(E, J_i, \pi_i) = \frac{1}{\sigma_i (2\pi)^{1/2}} exp[-(E - E_i)^2/2\sigma_i^2] B(E, J_i, \pi_i) f(Q_\beta - E) \tag{3}$$

with integrated Fermi function

$$f(Q_\beta - E) = \int_1^{E_0} F(Z, \epsilon)\epsilon\sqrt{(\epsilon^2 - 1)}(E_0 - \epsilon)^2 d\epsilon.$$

$T_f(E, J_i, \pi_i)/T_{\rm tot}$ denotes the fission probability of the compound nucleus:

$$\frac{T_f(E, J_i, \pi_i)}{T_{\rm tot}(E, J_i, \pi_i)} = \{1 + \left(\frac{T_n(E, J_i, \pi_i) + T_\gamma(E, J_i, \pi_i)}{T_{\rm eff}(E, J_i, \pi_i)}\right)^2 + \tag{4}$$

$$2 \cdot \frac{T_n(E, J_i, \pi_i) + T_\gamma(E, J_i, \pi_i)}{T_{eff}(E, J_i, \pi_i)} \cdot \coth[\frac{T_A(E, J_i, \pi_i) + T_B(E, J_i, \pi_i)}{2}]\}^{-\frac{1}{2}}$$

where

$$T_{\rm eff} = \frac{T_A(E, J_i, \pi_i) \cdot T_B(E, J_i, \pi_i)}{T_A(E, J_i, \pi_i) + T_B(E, J_i, \pi_i)} \ ,$$

with

$$T_{A,B}(E,J,\pi) = \int_0^E \rho_{A,B}(\epsilon,J,\pi) T_{HW}(E - E_{A,B} - \epsilon - h^2 l(l+1)/2\theta, h\omega_{A,B}) d\epsilon \ . \quad (5)$$

T_{HW} denotes the Hill-Wheeler [25] transmission coefficient through a parabolic barrier

$$T_{HW}(E, h\omega) = \frac{1}{1 + exp(-2\pi E/h\omega)} \quad , \quad (6)$$

and the available energy is reduced by the rotational energy with the moment of inertia θ deduced from the irrotational flow model [26]. The fission barrier heights $E_{A,B}$ will be discussed in Section 3. $\rho_{A,B}$ define the level densities above the first and second saddle points, which show an enhancement over the level densities at ground state deformation, due to increased deformation and coupling to low-lying rotational excitations. This enhancement is larger for the first axially asymmetric barrier than for the second mass asymmetric barrier. As in previous calculations, we used constant enhancement factors 4 or 2, respectively, over the level density at ground state deformation [27,28].

The back-shifted Fermi-gas description of the level density was improved by introducing an energy dependent level density parameter a as described in ref.[23]. Tests show a very good agreement with shell model calculations [29] and justify the application at and above the neutron separation energy.

The amount of experimentally known fission barriers used in the present calculations was increased recently by approximately a factor of 2 following the IAEA-report [27] and recent compilation in [13].

The relative probability of beta-delayed fission over pure beta-decay is $P_{\beta df} = \lambda_f/\lambda$ where λ denotes the β-decay rate, obtained from Eq. (5) without the term $T_f/T_{\rm tot}$.

2.2 Beta-strength function

The beta-strength functions, defined as

$$S_\beta(E) = \sum_i \beta_i(E, J_i, \pi)$$

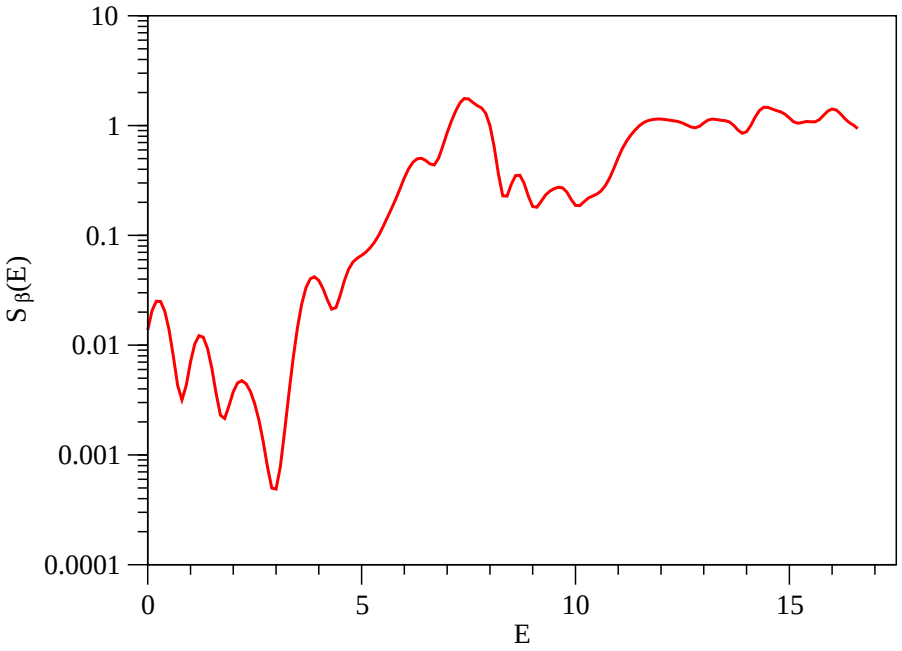

Fig. 3. Theoretical $S_\beta(E)$ for ^{300}U

for our calculations were derived on the basis of the QRPA calculations of reduced transition probabilities $B(E, J_i, \pi_i)$ [31] (see formula (3)).

In our calculations of beta-delayed fission probabilities we used the new approach for the beta-strength function [31], based on the approach [30], considered allowed transitions and deformed single-particle model as in [32] and takes into account the residual interaction. The model [31] combines calculations within the quasi-particle RPA for the Gamow-Teller part with an empirical spreading of quasi-particle strength and the gross theory for the first-forbidden part of β-decay.

In total fission barriers, penetrabilities/widths of all competing branches of the compound nucleus after beta-decay, and the beta strength functions are required to beta-delayed fission.

$P_{\beta df} = \lambda_f/\lambda$ using Eq. (2) can be written as

$$P_{\beta df}(Z,A) = \frac{\int\limits_0^{Qb} S_\beta(E)\frac{T_f}{T_{\rm tot}}dE}{\int\limits_0^{Q_b} S_\beta(E)dE} \qquad (7)$$

To calculate β-decay Q-values and neutron separation energies the experimental ground-state masses were used where available, otherwise calculated masses (ETFSI [33], Thomas-Fermi [2] or Howard and Möller [1]). To reduce

the uncertainties in the beta-strength function calculation due to uncertainties in individual level energies, a spreading of individual resonances were introduced above E=2 MeV. Specifically, each "spike" in the beta-strength function above 2 MeV was transformed into a Gaussian with width ≈ 0.5. The calculations were based on ground state deformations which affect the energy levels and wave-functions that are obtained in the single-particle model. The ground-state deformations were calculated in the FRDM mass model [34]. In some cases the first-forbidden strength calculated in the gross theory [35] was included.

The example of beta-strength function for the decay of ^{300}U is shown in (Fig. 3).

2.3 Cascade Model for secondary fission

All heavy nuclei near the r-process path are very neutron rich. Therefore the neutron separation energies for the daughter nuclei, produced in beta-decay, are very low. As a result, the probability of beta-delayed neutron emission can be high, frequently higher than probability of beta-delayed fission, (depending on fission barrier value). Therefore the excited states of a daughter nucleus produced by the beta-decay of neutron rich transuranium nuclei, mainly decay by neutron emission or fission. If neutron emission is the dominant decay mode it can lead to excited states that lie above the respective fission barrier and fission could occur in the second decay-step. This probability of secondary fission - $P_{\beta dnf}$, i.e., fission of the compound nucleus that is produced by neutron emission of the excited state of the daughter nucleus, will contribute to the total fission probability $P^{tot}_{\beta df}$ and might even enhance it significantly:

$$P^{\mathrm{tot}}_{\beta df}(Z,A) = P_{\beta df}(Z,A) + P_{\beta dnf}(Z,A) \tag{8}$$

The previous calculations [10,17] showed that $P_{\beta dnf}$-values can in certain cases be larger than $P_{\beta df}$-values, especially for neutron-rich isotopes of the Am-Cf region. In Fig. 2 some of the former results were shown for the mass relations of Hilf et al. [22] and fission barriers of ref. [1] (Fig. 4).

In order to evaluate the role of secondary fission on the base of new data this process can be investigated by iterating the SMOKER-code: if neutron emission leads to an excited level of the residual nucleus, we again calculate the branching ratios for the subsequent decay with the statistical model including the fission channel. Thus the probability for fission in the second decay step is essentially given by multiplication of the branching ratios for neutron emission and fission of the residual nucleus. Note that this is done by keeping track of

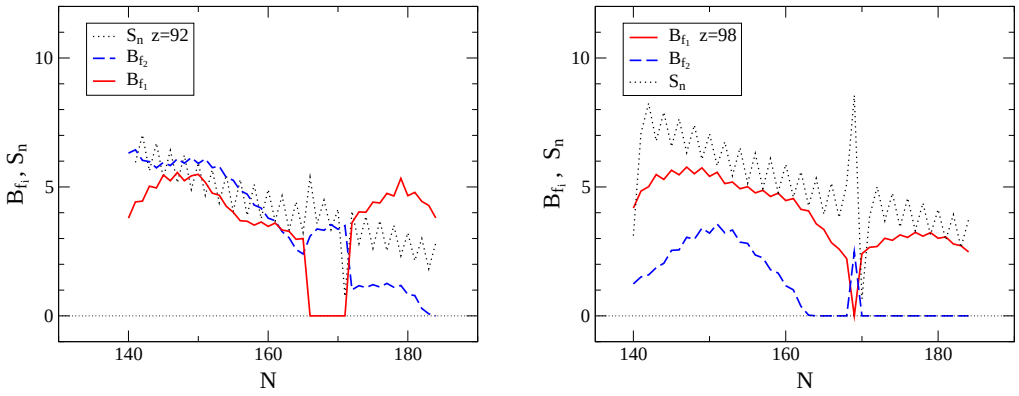

Fig. 4. The neutron separation energies (line) and fission barriers (dotted line) for U (left) and Cf (right) isotopes on the base of Howard and Möller (1980) approach.

energies, angular momenta and parities of the excited states, and the final probability for (β^-, nf)-decays is obtained by summing up the contributions from all quantum mechanically allowed partial waves.

Since the amount of excitation energy in the system is significantly reduced with every particle emission and eventually drops below the particle emission thresholds or fission barrier, we found that the cascade, could practically be terminated after two emission steps, contrary to neutrino-induced fission [37] when some subsequent emissions of different particles can occur. Thus, the residual daughter nuclei after two iterations were assumed to be in their ground state.

The significant values of fission probability after beta-delayed neutron emission (second step of cascade fission) - $P_{\beta dnf}$ can be reached only for the beta-decay with small beta-delayed fission probability $P_{\beta df}$ (first step of the cascade) and rather high beta-delayed neutron emission probability $P_{\beta dn}$ of mother nucleus. Especially high values of fission probabilities after neutron emission (second step of the cascade) can be achieved during decay of even-even mother nuclei (A,Z), when neutron separation energy in final nucleus (Z+1,A-1) significantly less than in daughter nucleus (Z+1,A) (See decay of U with A-266, 268, 270, Table 1 in Section 4.2.2).

3 Survey of fission barrier and mass predictions

As astrophysical applications include unstable nuclei not yet attained by experiment, all physical quantities have to be obtained from theoretical predictions. The quantities, which need to be employed for the calculation of neutron-induced and beta-delayed fission include the reaction Q-values and the fission barrier heights. For stable nuclei, this information can come from the experiment, but for unstable nuclei one has to make use of a mass formula

and theoretical predictions of fission barrier heights.

In addition to the Q-values and fission barriers involved, neutron emission and beta-decay require the knowledge of neutron optical potentials and beta strength functions. The accuracy of all these quantities strongly influences the probabilities of beta-delayed fission [11,18,21,36]. Several predictions exist so far, but their results differ strongly due to uncertainties for beta-strength functions and fission barriers of very neutron-rich and especially for deformed nuclei.

Fig. 2 and Fig. 4 show the connection between fission barriers and neutron separation energies on the one hand and fission probabilities, on the other hand, when Howard and Möller predictions were used. When fission barriers are of the order of neutron separation energy or become smaller than S_n, $P_{\beta df}$ increased and reached high values.

We also considered two different up-to-date fission barrier predictions, developed during recent years: one being based on the Thomas-Fermi model [2] and another using the Extended Thomas-Fermi model (ETFSI) [13]. Both the predictions, used in our calculations, include also the shell corrections. The analysis of fission barriers, predicted by these approaches, shows that the earlier fission barriers calculated by Howard and Möller [1] are systematically underestimated.

Fission barriers of the ETFSI model [13] made use of the (c,h)-parametrization [38] (see detailed explanation also in [28]). According to the ETF-predictions, fission barrier values increase with increasing N and that is why ETFSi predictions [13] show significantly greater fission barrier values than the MS calculations [2] due to several reasons, mentioned in [3,13]. The shell corrections due to the second term of total energy based on Strutinsky Integral can even increase the values for nuclei with magic numbers.

The accuracy of fission barrier predictions for large neutron excesses is hard to evaluate, and its effect on r-process results has to be studied.

The second approach [2] is based on self-consistent, semiclassical mean-field solution of the problem of self-bound nucleons interacting by suitably adjusted effective forces. This modification of Thomas-Fermi model of nuclei has been applied to the calculation of nuclear masses and fission barriers. To predict fission barriers in a range of N and Z of interest a simple algebraic expression was proposed. Predicted fission barriers include also the shell corrections (shell-correction method is described in [34]). The comparison with known experimental data shows the good agreement with calculations and one hopes the extrapolations of fission barriers are also reliable.

In Fig. 5, the neutron separation energies, as well as fission barriers for U and

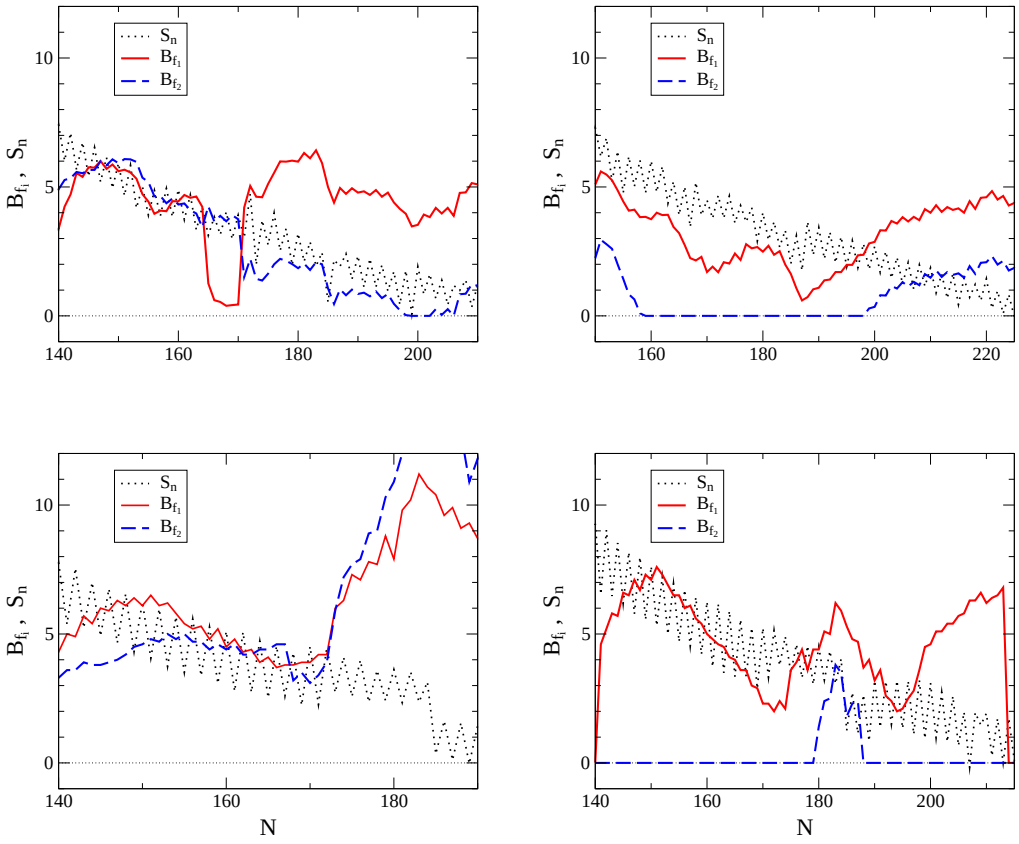

Fig. 5. The neutron separation energies (thin dotted line) and fission barriers (solid dashed line)of daughter nuclei under beta-decay of U (left) and Cf (right) isotopes on the base of different barrier predictions [2] (upper row) and [13] (low row).

Cf isotopes, calculated from considered mass relations, are shown. As it can be seen from the figure (the common features are the same for all actinides), the change of barrier heights as a function of neutron number is very similar for the different approaches, but differs strongly, especially for N $\approx$ 184, where Mamdouh et al. [13] show the absence of deformation and increasing barriers in excess of 10 MeV. The older mass formula of Hilf et al. [22], often used for astrophysical applications, predicts significantly smaller neutron numbers for the position of the neutron drip line than refs [1,2]. This has important implications, because in self-consistent calculations the r-process path can pass nuclei with larger neutron excess. For the region of interest, $A > 250$, the differences in S_n can be larger than 1 MeV.

While the agreement for experimentally known isotopes is quite good, the discrepancies of the approaches in the extrapolated region can achieve some MeV. These uncertainties can affect strongly the fission rates and the r-process. Therefore self-consistent calculations, predicting neutron separation energies, barriers and other nuclear properties on the same basis of the same hopefully reliable mass model are needed.

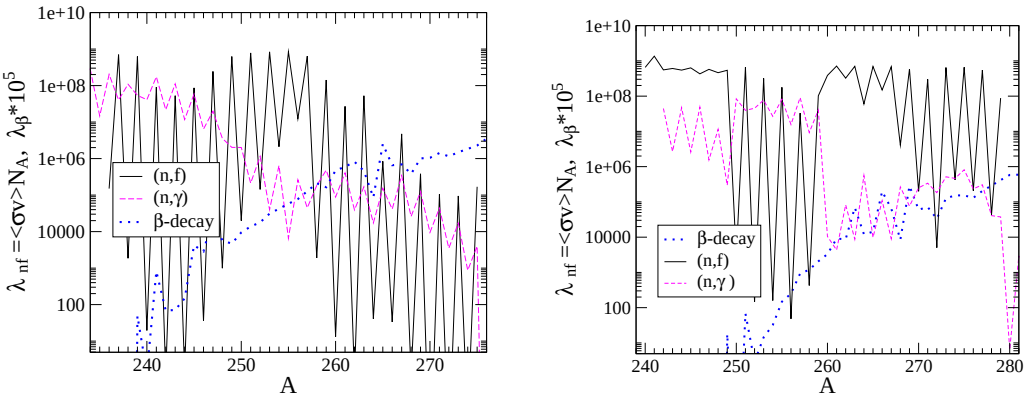

Fig. 6. The values of (n,γ), (n,f) and β-decay rates (in s^{-1}) for U (left) and Cf isotopes.

The preceding discussion (see also [48]) leads us to the conclusion that the fission barrier predictions from [1] underestimate whereas those from [13] overestimate the barrier at least in the vicinity of N $\approx$ 184. A main problem that arises when utilizing the barriers of ref. [2] lies in the fact that only the maximum barrier height is given while our calculations are based on the double-hump representation of fission [24]. In that case we estimated the height of the second barrier due to barrier differences from former calculations [1]:

$$B_{f_1} = B_f([2]);\;\; B_{f_2} = B_f([2]) - \Delta;\;\; where \;\; \Delta = B_{f_1}([1]) - B_{f_2}([1]) \quad (9)$$

Before applying the new fission rates to nucleosynthesis, we will evaluate the importance of individual contributions from different fission processes, i.e. beta-delayed fission versus neutron-induced fission and their dependence on different mass excess and fission barriers predictions.

4 Results

The approach described above was employed for the calculations of neutron-induced fission rates for neutron-rich isotopes up to the neutron-drip line, as well as beta-delayed fission rates for all isotopes of U, Pu, Am, Cm and Cf with beta-decay energies $Q_\beta > 0$.

4.1 The competition of different decay channels in the transuranium region

When the r-process approaches the actinide region, fission channels appear. Beta-delayed fission, proposed by Berlovich and Novikov [39], competes with beta-delayed neutron emission and pure beta-decay. Also the well known pro-

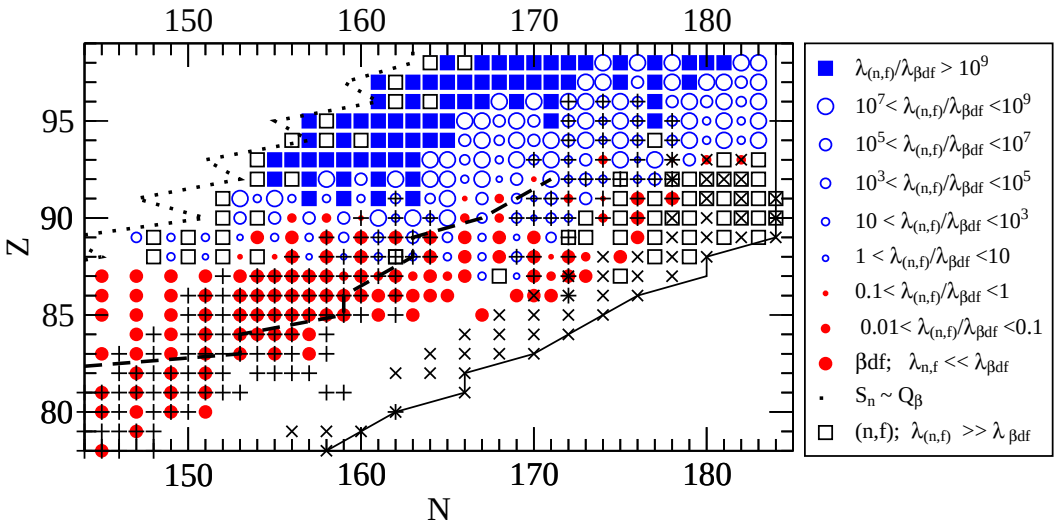

Fig. 7. The map of rates ratios $\lambda_{n,f}/\lambda_{\beta df}$ for $\rho Y_n = 1$ and $T_9 = 1$. The most abundant nuclei along the r-process path, for $n_n \approx 10^{26}$ (crosses), and $n_n \approx 10^{19}$ (pluses) are marked. The position of the neutron drip-line (full line), nuclei with neutron separation energy $S_n \approx 2MeV$ (dashed line) and nuclei with beta-decay energies $Q_\beta \sim S_n$ (dotted line) are denoted as well. These results were obtained for the mass model of Hilf et al. [22] and fission barriers by Howard and Moller [1].

cess of neutron induced fission has to be included. This process, discussed earlier [11] for uranium isotopes has not yet been included in r-process calculations. Neutron-induced fission rates can be very high for isotopes of transuranium elements and exceed beta-decay rates by orders of magnitude even near the neutron drip-line. This is mainly the case for very high neutron densities n_n as the product $< \sigma_{nf} v > n_n$ competes with beta-delayed fission rates $\lambda_{\beta df}$. The recycling timescale, measuring the time until the neutron capture on fission products leads again to the formation of actinides can be significantly less than the duration time of the r-process. The different rates for U and Cf isotopes are compared in Fig. 6. The rates in that Figure are given for $\rho Y_n = 1$ and $T_9 = 1$, the beta-decay rates are multiplied by 10^5. It is clear that for $\rho Y_n > 10^{-5}$ and for nuclei with $A > 250$ neutron-induced fission is more important than beta-delayed fission and radiative neutron-capture.

For the neutron-star merger scenario [41,42] or polar jets in supernova [40] such conditions are maintained for a long time ($\sim 1s$). However, as already pointed out above, the fission barriers of Howard and Möller [1] are very likely underestimated.

The calculation of rates for neutron-induced fission and beta-delayed fission made use of the statistical model code SMOKER, extended by including fission channels [11,36] as discussed in section 2.

A comparison of beta-delayed and neutron-induced fission rates calculated with fission barriers of Howard-Möller [1] is presented in Fig. 7, where circles and squares of different sizes indicate different ratios of rates. One can see that for $Z \leq 87$ the beta-delayed fission channel is the dominating one. For $Z = 88 - 90$ neutron-induced and beta-delayed fission are in competition, and for $Z > 91$ neutron-induced fission dominates. The open squares indicate nuclei for which the beta-delayed fission rate is equal to zero. For the neutron rich nuclei ($N > 160$) this is due to the small neutron separation energies ($S_n < B_f$) where the decay of a daughter nucleus occurs via neutron emission rather than fission (because the majority of beta-decay transitions goes through low lying states). The most abundant isotopes with Y(A,Z)> 1% Y(Z) (crosses) are shown for the early stages for the r-process (when $n_n > 10^{26}$) and the time when the neutron density decreases to less than 10^{20} (pluses).

Neutron-induced fission should be of significant importance for nuclei with the fission barrier $B_f \sim S_n$ or smaller and when the density of free neutrons is rather high. The rates of induced fission are large [11], [12], [43], and even for higher fission barriers [2,13] this branch of fission can be important. Preliminary calculations will be discussed below.

As already mentioned, in the majority of the r-process calculations fission was included in a very simple way: assuming 100% fission at given mass number A or charge number Z in the r-process path [7,8,9]. These simplified models permitted to investigate the behavior of nuclei formation due to cycling but affect the accuracy of nuclear abundances, in part, especially cosmochronometer yields [7,8,9].

The influence of a fission model in any astrophysical r-process scenario becomes important when the duration time τ_r of the r-process becomes larger than the fission cycling time $\tau_{\rm cycle}$. In this case, the r-process can successfully reach the transuranium region and all fission rates, beta-delayed, and neutron-induced as well as spontaneous fission, should be taken into account. In case of an artificial termination of the r-process for $A = A_{\rm max}$, the nuclei formed far beyond uranium undergoing α-decay will have incorrect abundances and will lead to wrong yields of cosmochronometer nuclei.

In some of the runs and in previous calculations [44] we took into account spontaneous fission only for nuclei with Z>92 and N>158 (according to known systematics) and we did not consider neutron-induced fission for these nuclei. In our calculations, even for highest fission barriers [3], the neutron-induced fission rates are sufficiently large to terminate or at least significantly reduce the build-up of higher Z r-process elements.

Simultaneous consideration of beta-delayed fission and neutron-induced fission in our calculation, and spontaneous fission in an other approach [45] give

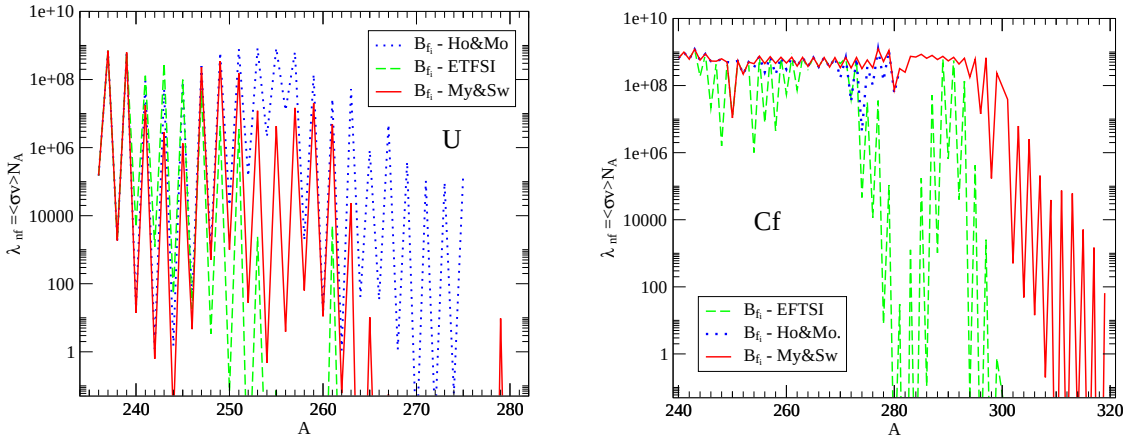

Fig. 8. Neutron-induced fission rates for U (left) and Cf (right) isotopes for different fission barriers as well as for different mass formulae.

very similar results (see Section 6), at least within the calculation accuracy. However, neutron-induced and beta-delayed fission should be faster and consequently more important in the r-process than spontaneous fission, which can play, however, an important role during cooling in the final decay of the r-process products.

But for a consistent inclusion of fission in the r-process, especially for the calculation of the final abundances, the specific scenarios of the r-process in very high neutron density environments should be considered.

4.2 Mass model dependence of fission rates

Here we present the neutron-induced fission rates and beta-delayed fission rates calculated for isotopes of some transuranium elements taking into account different up-to-date fission barriers and atomic mass predictions.

4.2.1 Neutron-induced fission rates

In Fig. 8, the neutron-induced fission rates λ_{nf} derived with the barriers of ref. [1] and mass predictions of [22] are compared with consistent calculations when all mass and fission barriers predictions were made on the base of approaches [46], [47]. The results show that for uranium isotopes with atomic masses A<260 the rates using Thomas-Fermi predictions [2] are also rather high whereas the rates calculated on the base of ETFSI predictions [13] for atomic masses greater 250 become too small compared to beta-decay and neutron capture rates. The latter can not interrupt the formation of new

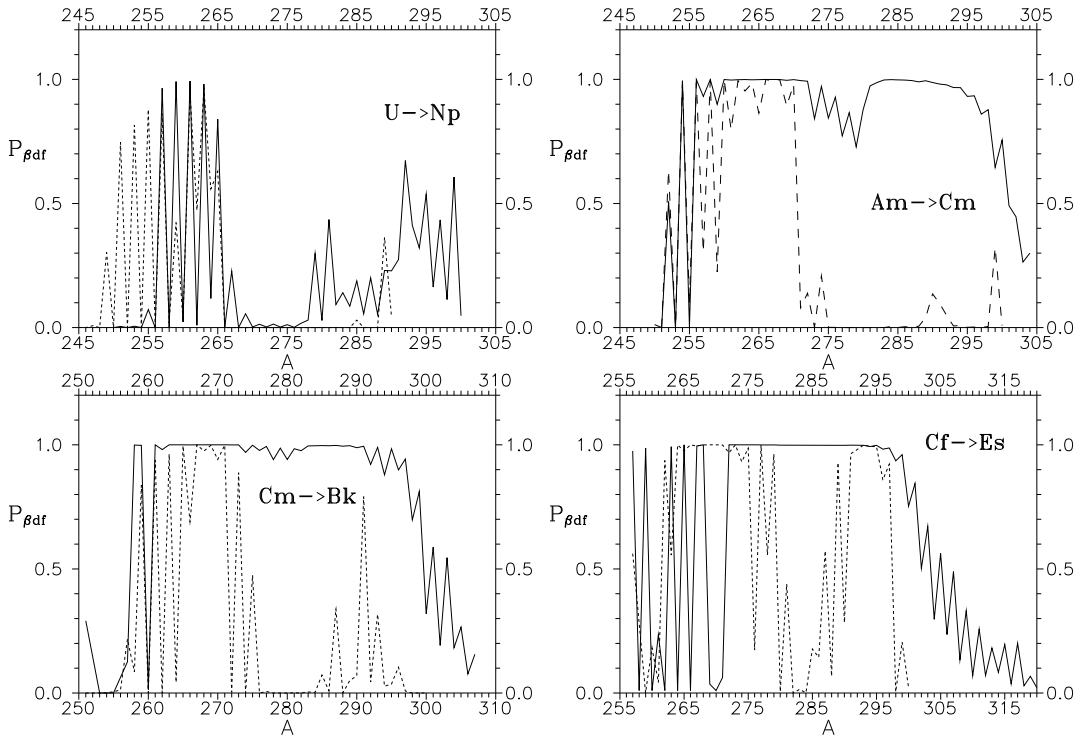

Fig. 9. Fission probabilities $P_{\beta df}$ for U, Am, Cm and Cf isotopes for mass models of Mamdouh et al. (Dashed line) and Myers and Swiatecki (line).

transuranium elements in r-process nucleosynthesis. As mentioned above the comparison was made for very high neutron environments with $\rho Y_n = 1$. As Z increases the rate values go up and all approaches give very high values of neutron-induced fission rates already for Cf isotopes, with the exception of the ETFSI approach in the vicinity of neutron shell N=184 (Fig. 8), where $S_n << B_f$. But the heights of barriers [13] for these nuclei seem to be overestimated [48].

4.2.2 beta-delayed fission rates

The first extended results for beta-delayed fission probabilities (Fig. 9) for the majority of neutron-rich isotopes of some chemical elements show that for fission barriers of refs. [2], [13], which are significantly higher then previously used [1], the values of $P_{\beta df}$ are still high for very neutron rich isotopes. For majority of them this applies in the case when mass model [2] was used and for part of them when the model based on ETFSI [3] was used.

Calculations of fission rates in the framework of the statistical model(see [10] and Section 2 of the present work) for both self-consistent approaches [13], [2] show similar results when the maximum values are reached for isotopes with atomic mass numbers A$\approx 255 - 265$. But with increasing Z the region of isotopes with high values of $P_{\beta df}$ close to 100% expands and in case of data

Table 1
Beta-delayed cascade fission probabilities (in %) for some U isotopes.[1)]

decay	A	$P_{\beta df}$	$P_{\beta n}$	$P_{\beta dnf}$	$P^{\rm tot}_{\beta df}$	$P^{\rm max}_{n\beta df}$	$P^{\rm min}_{n\beta df}$
U →Np	264	41	59	4	45	86	-
U →Np	266	8	92	69	77	38	-
U →Np	268	1	99	28	29	25	7
U →Np	270	3	96	23	26	44	14
U →Np	272	3	97	8	11	23	10
U →Np	274	4	96	4	8	16	11
U →Np	276	2	98	9	10	31	-

[1)] $f P^{\rm tot}_{\beta df}$(Z,A)$=P_{\beta df}+P_{\beta dnf}$, $\quad P^{\rm max}_{\beta dnf}\equiv P_{\beta df}(Z+1,A-1)$,

set [2] the majority of isotopes attain close to maximum values above Z=95 and in case of [13] above Z=98. The suppression in $P_{\beta df}$ values for californium for the ETFSI barriers is explained by very high fission barriers in the vicinity of nuclei with number of neutrons close to 184.

In Table 1, the results of the cascade calculations for beta-delayed fission are shown. We present the results of the calculations for the nuclei with very small values of direct beta-delayed fission probability $P_{\beta df}$. As it was expected the fission probability after delayed neutron emission $P_{\beta dnf}$ can be high. For some decays total $P^{\rm tot}_{\beta df}$ which is the sum of beta-delayed fission (first step of cascade fission) and fission after beta-delayed neutron emission (second step of cascade) increases by several times. That means, that the cascade mechanism can be important for nuclei for which the direct (one step) beta-delayed fission is small and beta-delayed neutron emission is high.

In the last two columns the results of our evaluations are presented. The first ($P^{\rm max}_{\beta dnf}$) shows the fission contribution during beta-decay of daughter nucleus. The second one ($P^{\rm min}_{\beta dnf}$) shoes the same but in assumption that compound nucleus does not changed during all the steps of cascade. It was calculated as probability of delayed fission of daughter nucleus but with reduced β-strength function of the mother nucleus $S_\beta(U)$ where $U=E-S_n$ as in [51]. Different mass and barrier predictions for U [1] and Cf [13] were used.

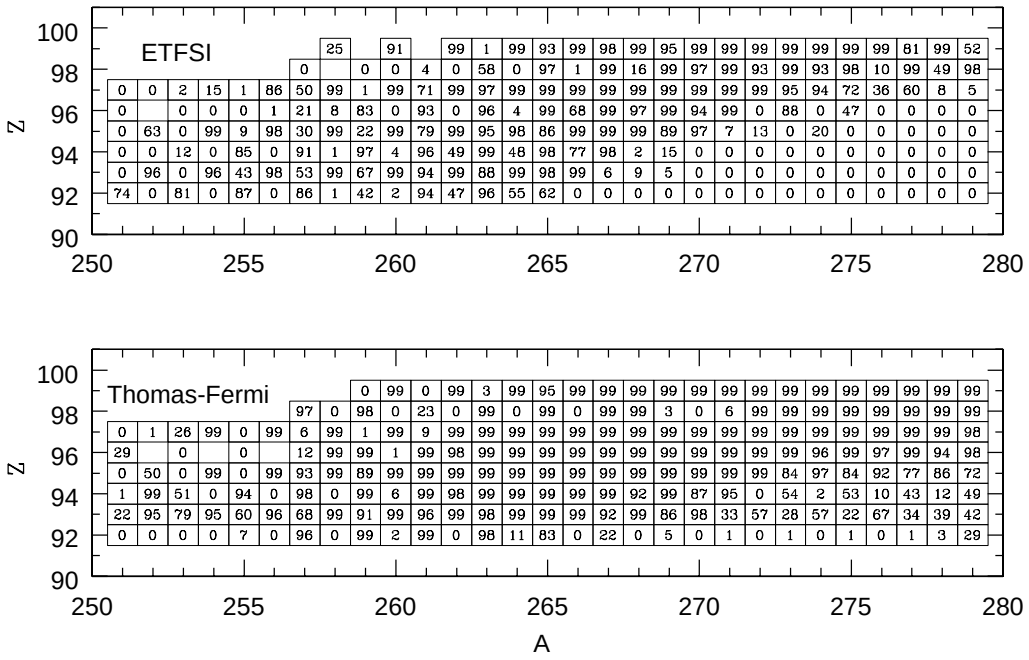

Fig. 10. ETFSI and Thomas-Fermi beta-delayed fission probabilities

5 Discussion and outlook.

5.1 Consequences of new rates utilization for the r-process)

The discrepancy of fission rates due to different mass predictions is high, especially for the region of nuclei with N $\sim$ 184, where different mass models predict different dependence of fission barriers on N. New efforts are needed to improve the models for better agreement, mainly in the region of nuclei with very big neutron excess so important for the r-process. It should be noted that the results of Hartree-Fock mass calculations [48] point out that ETFSI-calculation [13] are overestimated, at least in the vicinity of N=184. That is why we can consider the fission rates of Howard and Möller [1] were underestimated, the rates based on ETFSI are overestimated. This assumption lets us discuss what can be expected when the fission rates are applied to the r-process calculations.

Looking at Fig. 10 and Table 2, it is clear that the beta-delayed fission probabilities are quite high for the majority of isotopes of transuranium elements, independent of differences in mass models and strength-function calculation.

When moderate neutron densities are considered ($n_n \sim 10^{22} - 10^{24}$ for tem-

perature of 1.3×10^9 K), the r-process passes through the region of nuclei with neutron separation energies $S_n \approx 2-3MeV$. Very high fission barriers, as predicted by some calculations [13] will not avoid an influence on the r-process, they only move the effective region to nuclei with atomic mass numbers A $\approx$ 260, where fission rates, particularly beta-delayed fission, are high (Fig. 9, Fig. 10). For very high neutron densities ($n_n >> 10^{24}$), when the path of the r-process lies closer to neutron drip line, beta-delayed fission rates for fission barriers by Mamdouh et al. [13] will be small. But neutron-induced fission rates can be significant for such conditions and additional calculations of the r-process are needed to clarify the question.

In every case of long neutron exposure (with durations of the r-process $\tau_r >> \tau_{\rm cycle}$), the r-process seeds capture on average more than 150 neutrons, thus moving high abundances to the end of r-process path, where the fission stops the formation of heavier nuclei. Due to fission, the fission products enter the r-process again at smaller mass numbers (r-process cycling). The termination of the r-process due to the fission occurs in the range of nuclei with charge numbers $92 < Z < 98$. Here, $\tau_{\rm cycle}$ - the time of r-process propagation from the average fission products to the transuranium region is defined as :

$$\tau_{\rm cycle}^{-1} = \sum_{Z_i} \lambda_\beta^i; \quad \lambda_\beta^i = \sum_j Y(Z_i, A_j) \cdot \lambda_\beta^j$$

For higher fission barriers a longer duration time is encountered and heavier nuclei are formed.

5.2 Possible role of triple/ternary fission in the r-process

Utilization of the latest calculations of fission barriers [2,13] should result in a decrease of fission rates in comparison to former barriers [1] previously used in r-process calculations. This in turn should lead to an increase of the maximum atomic numbers of fissioning nuclei formed in the r-process in excess of Z$\approx$96.

In comparison to the Hilf et al. mass formulae [22], recent consistent approaches shift the neutron drip line in the direction of heavier masses. For example, the mass prediction of Hilf et al. [22] defines the atomic mass of the heaviest Cf isotope to be A=279, while the other calculations discussed above [2,13] predict the existence of Cf isotopes heavier than A=300. The widening of the r-process region can result in a shift of the r-process path into the direction of larger atomic mass numbers. In case of r-process environments with moderate neutron densities binary fission leads to an abundance curve downing strongly below $A \sim 130$ due to cycling of the r-process after all lighter

Table 2
Beta-delayed fission probabilities for U and Cf isotopes.

U	$HoMo^{*1)}$	$HoMo$	$MsSw$	ETFSI	Cf	$HoMo^{*1)}$	$HoMo$	$MsSw$	ETFSI
250	0	0	0	0	260	0	0	01	0
251	86	86	0	74	261	0	4	23	4
252	22	33	0	00	262	0	0	01	0
253	94	94	01	81	263	08	71	99	58
254	71	76	0	0	264	01	05	01	00
255	98	99	08	88	265	80	99	99	97
256	91	94	0	0	266	83	87	01	01
257	99	99	96	88	267	95	99	99	99
258	89	96	00	03	268	90	99	99	16
259	98	98	99	75	269	91	99	04	99
260	40	93	03	01	270	81	99	01	97
261	95	99	99	96	271	88	99	06	99
262	15	88	01	12	272	72	99	99	93
263	86	97	96	98	273	85	99	99	99
264	38	6	12	73	274	77	97	99	93
265	37	97	83	76	275	88	99	99	98
266	26	91	00	00	276	69	80	99	10
267	24	97	20	01	277	81	99	99	99
268	01	27	00	0	278	81	99	99	49
269	44	94	05	0	279	86	99	99	98
270	05	32	00	0	280	88	99	99	01
271	23	85	01	0	281	86	99	99	84
272	05	35	00	0	282	87	99	99	00
273	16	60	01	0	283	89	99	99	05
274	03	38	00	0	284	-	-	99	00
275	30	74	01	0	285	-	-	99	98
276	07	37	00	0	286	-	-	99	99
277	46	97	02	0	287	-	-	99	99
278	-	-	03	0	288	-	-	99	20

[1)] Mass predictions were made according to ref. [22]

nuclei have vanished due to neutron capture. For very high neutron density environments, when the r-process passes partly along or very close the neutron drip-line, the mass of light fission fragment can be greater than 130. Such a mass distribution of fission fragments could affect the good agreement of calculations and observation of heavy element abundances when using binary fission only.

Triple or ternary fission [16,49,50] can populate nuclei with $A < 130$ and should be considered as well. It can save the agreement with observations, but to define the exact contribution of triple fission into the r-process the extended nucleosynthesis calculations should be done.

Ternary and quaternary fission are observed experimentally [52]. Theoretical evaluations of the possibility of fission into n equal fragments (ternary fission when $n = 3$) followed [53]. For example, when the fissility parameter exceeds 0.61 (that is usual for neutron rich transuranium nuclei), ternary fission energetically becomes more preferable to binary fission.

Of course, the probability of triple fission of long lived or experimentally known nuclei is small because of the high second barrier of ternary fission and long path to the saddle point of ternary fission in comparison with binary fission. The experimental evaluation of the ternary fission probability in neutron induced reactions at low energy shows that this process is at least by 3 orders smaller than binary fission and the formation probability of a heavy third fragment (A$>$ 40) decreases below 10^{-6} [50]. The latest extended experiment using the FOBOS-detector [54] shows that fission yields for three fragments with $Z > 20$ are approximately 10^{-3} lower than the binary ones in the nuclear system formed in the $^{14}N +^{234} Th$ collision. In forthcoming experiments the ternary yields in the decay of nuclei with larger Z^2/A will be measured [54]. But experiments with heavy ions [49] show that the yield of ternary fission fragments of stable or long-lived isotopes of Th, U and Bi can be of the same order as in binary fission. The masses of ternary fragments were approximately equal.

Up to now there are no theoretical predictions for ternary fission of unstable neutron-rich nuclei involved in the r-process [16]. According to the theory of ternary fission, fission into three fragments occurs if reach the quasi-stable ternary valley [16], which is difficult to investigate experimentally because of the high second barrier. But with increasing atomic number and probably neutron number, the second barrier of the ternary valley decreases, especially when the lightest third fragment A_3 is significantly heavier than alpha-particles, and the probability of ternary fission increases.

All these experimental facts and theoretical evaluations let us consider that after beta-delayed fission of extremely neutron rich nuclei (when the energy of

beta-decay is about 15 MeV or more and is of the order of shell corrections), the probability of ternary fission of nuclei with fissility $x > 0.61$ can be rather high.

In the extreme case when ternary fission of very neutron rich nuclei is strong, many intermediate nuclei can be formed in the r-process and the impact of such a fission process upon the yields of intermediate r-elements should be investigated.

At least two extreme cases can be discussed:

1) true ternary fission into 3 approximately equal fragments (quatro fission occurs when $x > 0.87$ and it is not considered, because the fissility values for neutron-rich nuclei involved in r-process lie mainly in the x=0.55-0.7 region).

2) triple fission when the average mass of the third fragment is small: $A_3 \sim 10 - 20$. In this case two other fragments should have smaller masses than in the case of simple binary fission because 10-20 mass units can be gathered in the third fragment. At least one heavy fragment will be included into the r-process before the $A = 130$ peak.

6 Summary

The new calculations of fission rates considered two consistent approaches. The calculations showed that, on a whole, the new rates based on fission barriers of [2,13] are lower than the ones previously used [10,12,43]. However, taking into account a cascade model of fission after beta-delayed neutron emission, the total value of fission rates can increase in some cases, especially when beta-delayed fission of the mother nucleus is low and primary beta-delayed neutron emission is high. For such nuclei the addition to delayed fission after neutron emission can be significant and the total value of beta-delayed fission can increase strongly.

Unfortunately, the agreement of different calculations (used in different mass and fission barrier predictions) have not converged yet, especially for very neutron rich nuclei in the region with N $\sim$ 184.

The extended calculations of fission rates taking into account Thomas-Fermi [2] and ETFSI [13] fission barriers have not been finished yet. A detailed comparative analysis of the influence of fission modes on the results of nucleosynthesis was made in full network calculations [43,55] using the mass relations [22] and fission barriers [1], used for years in many astrophysical applications. An evaluation of the relative contribution of neutron-induced and β-delayed

fission on the formation of r-elements under conditions of high neutron densities ($10^{20} < n_n < 10^{30}$) was made. Our present calculations of fission rates should not change significantly our previous conclusions concerning competition of beta-delayed fission and neutron induced fission but the resulting changes in r-process abundances can be significant.

The calculation of the yields Y(A) for the range of atomic masses $120 < A < 240$ depend weakly on the model of the fission approximation. For predicting the yields of nuclei heavier than 240, especially nucleo-cosmochronometer yields and abundances of intermediate nuclei with atomic mass numbers $100< A <120$, fission should be included as precisely as possible. Nuclei lighter than 120 can be formed if the fission of many transuranium nuclei is mainly asymmetric. To consider all the opportunities, a schematic model for the mass distribution [44], including both symmetric and asymmetric [56] fission was applied earlier.

In the classical model of the r-process, the r-process path proceeds under moderate free neutron densities and close to nuclei with a neutron separation energy $S_n \approx 2$MeV, for which in the transuranium region the values of beta-delayed fission are the highest ones. According to the existing fission probability calculations $P_{\beta df}$ [10,17], based on old fission barrier predictions [1], the r-process would stop in the region of transuranium nuclei at atomic mass numbers A $\approx$ 250-260 and charge Z $\approx$90-96. In that case, the approximation of 100% instantaneous fission in the vicinity of A$\sim$260 (for simplicity A=260) used in [6,9,11] would be quite good. However, new fission rates can change the termination point of the r-process to the region of A $\approx$ 260-280 and Z $\approx$94-98.

When considering dynamical r-process models at extremely high neutron densities, in which fission occurs strongly, the path of the r-process lies close to neutron drip-line, and the efficiency of beta-delayed fission depends strongly on fission rates for the group of nuclei close to the neutron shell N$\approx$184. In particular, in the scenario realized in the model of neutron star mergers [41], [42], r-process nucleosynthesis proceeds mainly along the neutron drip-line [57] due to very high neutron densities. In this case, the role of neutron-induced fission will be comparatively more important than beta-delayed fission. For realistic fission barriers [2,13] and mass predictions [46,47], nuclei with masses as large as A$\sim$300 could be formed. In this case the predicted abundance curve for nuclei below $A \sim 130$ should also consider triple (ternary) fission.

The probability of triple (or ternary) fission [49,50] is highly uncertain but for nuclei with $A > 260$ near the neutron drip-line, fission into 3 fragments is energetically possible and could occur. Present [50] and forthcoming [58] experiments should clarify the probabilities of such a processes.

For the development of the r-process models a detailed analysis of fission properties is required. Except for neutron-induced fission and β-delayed fission, neutrino-induced fission was also proposed recently [59]. In this connection one should notice that neutrino rates [60] can also have great importance for specific astrophysical conditions. Precise fission rates and mass fragment distributions after fission have to be obtained and included in r-process calculations.

After extended calculations of both beta-delayed fission probabilities and neutron-induced fission rates for all nuclei involved in the r-process, we hope to clarify the question of the role of fission rates at different stages of nucleosynthesis for more specific astrophysical conditions. Due to our new results (see Fig. 10), it seems that fission will affect the r-process, but further detailed studies are ahead.

Acknowledgements.

The authors thanks F. Gönnenwein, S. Goriely, C. Wagemans and all colleagues, especially participants of the Conferences: Nuclei in the Cosmos (Tokyo, 2002), Seminar on Fission (Pont d'Oye, 2003), Nucleus-2003 (Moscow 2003) for discussions on fission data, especially mass distribution of fission fragments.

This work supported by grant 20-68031.02 of the Swiss National Science Foundation and partially supported by grant 04-02-16793-a of Russian Foundation of Basic Research (RFBR).

References

[1] W.M. Howard, P. Möller, ADNDT, 25 (1980) 219.

[2] W.D. Myers, W.J.Swiatecki, Phys. Rev. C 60 (1999) 014606-1.

[3] A. Mamdouh, J.M. Pearson, M. Rayet, F. Tondeur, Nucl. Phys. A 644 (1998) 389.

[4] P.A. Seeger, W.A. Fowler, D.D. Clayton, Astrophys. J. Suppl. 97 (1965) 121.

[5] J.J. Cowan, F.-K. Thielemann, J.W. Truran, ApJ **323** (1987) 543.

[6] J.J. Cowan, B. Pfeiffer, K.-L. Kratz, F.-K. Thielemann, C. Sneden, S. Burles, D. Tytler, T.C. Beers, Astrophys. J. 521 (1999) 194.

[7] V.M. Chechetkin, Yu.S. Lyutostansky, S.V. Malevanny, I.V. Panov, Sov.J. Nucl. Phys. (USA) 47 (1988) 780.

[8] C. Freiburghaus, J.-F. Rembges, T. Rauscher, E. Kolbe, F.-K. Thielemann, K.-L. Kratz, B. Pfeiffer,J.J. Cowan, Astrophys. J. 516 (1999) 381.

[9] T. Rauscher, J.H. Applegate, J.J. Cowan, F.-K. Thielemann, M. Wiescher. Astrophys. J. 429 (1994) 499.

[10] F.-K. Thielemann, J. Metzinger, H.V. Klapdor-Kleingrothaus, Zt. Phys. A 309 (1983) 301.

[11] F.-K. Thielemann, A.G.W. Cameron, J.J. Cowan, Proc. of Int. Conf. 50 years with Nuclear Fission, 1989, ed. J. Behrens, A.D. Carlson, p. 592.

[12] I.V. Panov, F.-K. Thielemann, Astronomy Lett. 29 (2003) 510.

[13] A. Mamdouh, J.M. Pearson, M. Rayet, F. Tondeur, Nucl. Phys. A 679 (2001) 337.

[14] G.J. Wasserburg, M. Busso, R. Gallino, Astrophys. J. 466 (1996) L109.

[15] I.V. Panov, C. Freiburghaus, F.-K. Thielemann, Nucl. Pnys. A 688 (2001) 587.

[16] H Diehl, W. Greiner, Nucl. Pnys. A 229 (1974) 29.

[17] A. Staudt, H.V. Klapdor-Kleingrothaus, Nucl. Phys. A 549 (1992) 254.

[18] I.V. Panov, Yu.S. Lyutostansky, V.I. Ljashuk, Bull. Acad. Sci. Ussr, Phys. ser. (USA) 54 (1990) 2137.

[19] A. Staudt, M.Hirsh, K.Muto et al., Phys. Rev. Lett. 65 (1990) 1543.

[20] H.V. von Groote, E.R. Hilf, K. Takahashi, ADNDT 17 (1976) 431.

[21] B.S. Meyer, W.M. Howard, G.J. Mathews, K. Takahashi, P. Moller, G.A. Leander, Phys. Rev. C 39 (1989) 1876.

[22] E.R. Hilf, H.V. Groote, K. Takahashi, Proc. 3 Int. Conf. on Nucl. far from Stability, 1976, CERN-76-13, 142.

[23] T. Rauscher, F.-K. Thielemann, K.-L. Kratz, Nucl. Phys. A 621 (1997) 331c.

[24] V.M. Strutinsky, Nucl. Phys. A 95 (1967) 420.

[25] D.L. Hill, J.A. Wheeler, Phys. Rev. 89 (1953) 1102.

[26] A. Bohr, B. Mottelson, Nuclear Structure, Vol. II (Benjamin, New York, 1975).

[27] G.N. Smirenkin, IAEA-report INDC(CCP)-359, 1993.

[28] S. Bjornholm, J.E. Lynn, Rev. Mod. Phys. 52 (1980) 725.

[29] D.J. DeanD, S.E. Koonin, K. Langanke, P.B. Radha, Y. Alhassid, Phys. Rev. Lett. 74 (1995) 2909.

[30] P. Möller, J. Randrup, Nucl. Phys. A 514 (1990) 1.

[31] P. Moller, B. Pfeiffer, K.-L. Kratz, Phys. Rev. C 67 (2003) 055802.

[32] J.Krumlinde, P.Möller, Nucl. Phys. A 417 (1984) 419.

[33] J.M. Pearson. R.C. Nayak, S. Goriely, Phys. Lett. B 387 (1996) 455.

[34] P. Moller, J.R. Nix, W.D. Myers, W.J. Swiatecki, ADNDT 59 (1995) 185.

[35] T. Kodama, K. Takahashi, Nucl. Phys. **A239**, 489 (1975).

[36] J.J. Cowan, F.-K. Thielemann, J.W. Truran, Phys. Reports 208 (1991) 267.

[37] A. Hektor, E. Kolbe, K. Langanke, J. Toivanen, Phys. Rev. C 61 (2000) 055803.

[38] M. Brack, J. Dangaard, A.S. Jensen, H.C. Pauli, V.M. Strutinsky, Rev. Mod. Phys. 44 (1972) 320.

[39] E.E. Berlovich, Yu.P. Novikov, Reports Academy of Science USSR. 185 (1969) 1025; Phys.Lett. B 29 (1969) 155.

[40] A.G.W. Cameron, Astrophys. J. 587 (2003) 327.

[41] C. Freiburghaus, S. Rosswog, F.-K. Thielemann, Astrophys. J. 525 (1999) L121.

[42] S. Rosswog, M. Liebendorfer, F.-K. Thielemann, M.B. Davis, W. Benz, T. Piran, Astron. Astrophys, 341 (1999) 499.

[43] I.V. Panov, F.-K. Thielemann, Nucl. Phys. A 718 (2003) 647.

[44] I.V. Panov, C. Freiburghaus, F.-K. Thielemann, Nucl. Phys. A 688 (2001) 587c.

[45] S. Goriely, B. Clerbaux, Astron. Astrophys. 346 (1999) 798.

[46] W.D. Myers, W.J.Swiatecki, Nucl. Phys. A 601 (1996) 141

[47] Y. Aboussir, J.M. Pearson, A.K. Dutta, F. Tondeur, ADNDT 61 (1995) 127

[48] S. Goriely, M. Samyn, P.-H. Heenen, J.M. Pearson, F. Tondeur, Phys. Rev. C 66 (2002) 024326.

[49] V.P. Perelygin, N.H. Shadieva, S.P. Tretiakova, A.H. Boos, R. Brandt, Nucl. Phys. A 127 (1969) 577.

[50] I. Tsekhanovich, Z. Buyukmumcu, M. Davi, H.O. Denschlag, F. Gonnenwein, S.F. Boulyga, Phys. Rev. C67 (2003) 034610.

[51] Yu.S. Lyutostansky, I.V. Panov, V.K. Sirotkin, Phys. Lett. B 161 (1985) 9.

[52] Tsien San-Tsiang, Ho Zan-Wei, R. Chastel, L. Vigneron, Phys. Rev. 71 (1947) 382.

[53] W.J. Swjatecky, Phys. Rev. 101 (1956) 651; 104 (1956) 993.

[54] C.-M. Herbach, D. Hilscher, V.G. Tishchenko, P. Gippner,D.V. Kamanin, W. von Oertzen, H.-G. Ortlepp, Yu.E. Penionzhkevich, Yu.V. Pyatkov, G. Renz,K.D. Schilling, O.V. Strekalovsky, W. Wagner, V.E. Zhuchko, Nucl. Phys. A 712 (2002), 207.

[55] I.V. Panov, F.-K. Thielemann, Astronomy Letters, 30 (2004) 8.

[56] M.G. Itkis, V.N. Okolovich, G.N. Smirenkin, Nucl. Phys. A 502 (1989) 243c.

[57] I.V. Panov, Astronomy Letters, 29 (2003) 163.

[58] Yu.N. Kopach, M. Mutterer, D. Schwalm, P. Thirolf, F. Gënnenwein, Phys. Rev. C 65 (2002) 04461.

[59] Y.-Z. Qian, Astrophys. J. 569 (2002) L103.

[60] K. Langanke, G. Martínez-Pinedo, Rev. Mod. Phys. 75 (2003) 819.